Identifying unique acoustic signatures from chemically-crosslinked microbubble clusters using deep learning

Pathour, Teja, Akter, Nasrin, Dormer, James, Chaudhary, Sugandha, Fei, Baowei, et al.

Teja Pathour, Nasrin Akter, James D. Dormer, Sugandha Chaudhary, Baowei Fei, Shashank Sirsi, "Identifying unique acoustic signatures from chemically-crosslinked microbubble clusters using deep learning," Proc. SPIE 12038, Medical Imaging 2022: Ultrasonic Imaging and Tomography, 120380K (4 April 2022); doi: 10.1117/12.2611572

SPIE.

Event: SPIE Medical Imaging, 2022, San Diego, California, United States

Identifying Unique Acoustic Signatures from Chemically-Crosslinked Microbubble Clusters Using Deep Learning

Teja Pathour [a], Nasrin Akter [a], James D. Dormer [a,b], Sugandha Chaudhary [a], Baowei Fei [a,b,c,*], Shashank Sirsi [a,b,*]

[a] Department of Bioengineering, The University of Texas at Dallas, TX
[b] Center for Imaging and Surgical Innovation, The University of Texas at Dallas, TX
[c] Department of Radiology, The University of Texas Southwestern Medical Center, Dallas, TX

* Corresponding authors: shashank.sirsi@utdallas.edu, https://labs.utdallas.edu/iddl/
bfei@utdallas.edu, https://fei-lab.org

ABSTRACT

Ultrasound contrast agents (UCA) are gas encapsulated microspheres that oscillate volumetrically when exposed to an ultrasound field producing a backscattered signal which can be used for improved ultrasound imaging and drug delivery. UCA's are being used widely for contrast-enhanced ultrasound imaging, but there is a need for improved UCAs to develop faster and more accurate contrast agent detection algorithms. Recently, we introduced a new class of lipid based UCAs called Chemically Cross-linked Microbubble Clusters (CCMCs). CCMCs are formed by the physical tethering of individual lipid microbubbles into a larger aggregate cluster. The advantages of these novel CCMCs are their ability to fuse together when exposed to low intensity pulsed ultrasound (US), potentially generating unique acoustic signatures that can enable better contrast agent detection. In this study, our main objective is to demonstrate that the acoustic response of CCMCs is unique and distinct when compared to individual UCAs using deep learning algorithms. Acoustic characterization of CCMCs and individual bubbles was performed using a broadband hydrophone or a clinical transducer attached to a Verasonics Vantage 256. A simple artificial neural network (ANN) was trained and used to classify raw 1D RF ultrasound data as either from CCMC or non-tethered individual bubble populations of UCAs. The ANN was able to classify CCMCs at an accuracy of 93.8% for data collected from broadband hydrophone and 90% for data collected using Verasonics with a clinical transducer. The results obtained suggest the acoustic response of CCMCs is unique and has the potential to be used in developing a novel contrast agent detection technique.

Keywords – Ultrasound contrast agent; Microbubble; Deep Learning; Bubble coalescence; Contrast-enhanced ultrasound

1. INTRODUCTION

Ultrasound contrast agents (UCAs), also known as "microbubbles", are used in contrast-enhanced ultrasound (CEUS) imaging due to their unique scattering properties [1]. UCAs are vascular contrast agents which enhance the scattered signal in the blood in ultrasound images. UCAs are used for cancer diagnosis and other biomedical applications [2-6]. However, despite recent advances in developing better ultrasound imaging techniques, there is still a need to improve the diagnostic accuracy of small and centrally located lesions in prostate cancer [7] and other cancer models. Some of the recent developments [7] improved diagnostic accuracies by using the subharmonic responses of UCAs produced by their nonlinear acoustic response. However, there are residual background noise that affect the image quality. We need better contrast agents that can be localized and detected with high signal to noise ratio.

Novel contrast agents produce unique acoustics that can be used for CEUS imaging, but the acoustic response might appear similar to conventional UCAs with traditional signal processing techniques as the distinction between the CAs may be hidden. With deep learning techniques, these hidden distinction and uniqueness of the novel CAs can be detected because of their special abilities to correlate and understand the hidden behavior of the acoustic responses. Detecting these novel acoustics will help in improving the image quality and resolution of CEUS imaging methods by improving signal to noise ratio.

Recently, our group has developed novel UCAs, called CCMCs [8]. Unlike individual UCAs, CCMCs are clusters that have a core and surrounding UCAs that are crosslinked to each other with copper-free click chemistry. CCMC's can coalesce

Medical Imaging 2022: Ultrasonic Imaging and Tomography, edited by Nick Bottenus, Nicole V. Ruiter,
Proc. of SPIE Vol. 12038, 120380K · © 2022 SPIE · 1605-7422 · doi: 10.1117/12.2611572

when exposed to low intensity pulsed ultrasound (US). We hypothesize that the coalescence of fused microbubbles will produce unique US backscatter that can be used for ultrasound imaging. Based on our hypothesis, we predict that the acoustic signature of CCMCs can be differentiated from traditional non-crosslinked individual UCAs, potentially leading to newer and more effective methods of contrast agent detection. The main purpose of this study is to investigate if the acoustic response of CCMCs is unique and can be differentiated from individual UCAs using deep learning.

2. METHODS

2.1 Preparation of CCMCs and Individual UCAs

Chemically cross-linked microbubble clusters are generated, similar to the method described by Hall et al[8], using copper-free click chemistry[9]. Briefly, two separate UCA samples with either DSPC-PEG5K-DBCO or DSPC-PEG5K-Azide are manufactured (the detailed procedure by Sirsi et al.[10]). Then these UCAs are mixed in a 1:10 (DBCO: Azide) ratio with fixed concentrations and incubated for one hour at 4 degrees Celsius. For the negative control, the DBCO-Azide chemistry is blocked using sodium azide, resulting in no cross-linking of bubbles. All the samples are validated using brightfield BX50 Upright Microscope (ACH 60X/0.80 ∞/0.17 objective) before moving on to data collection. Clusters are observed in CCMCs (Fig.1a) and individual UCAs are observed in the negative control (Fig 1b) under a microscope.

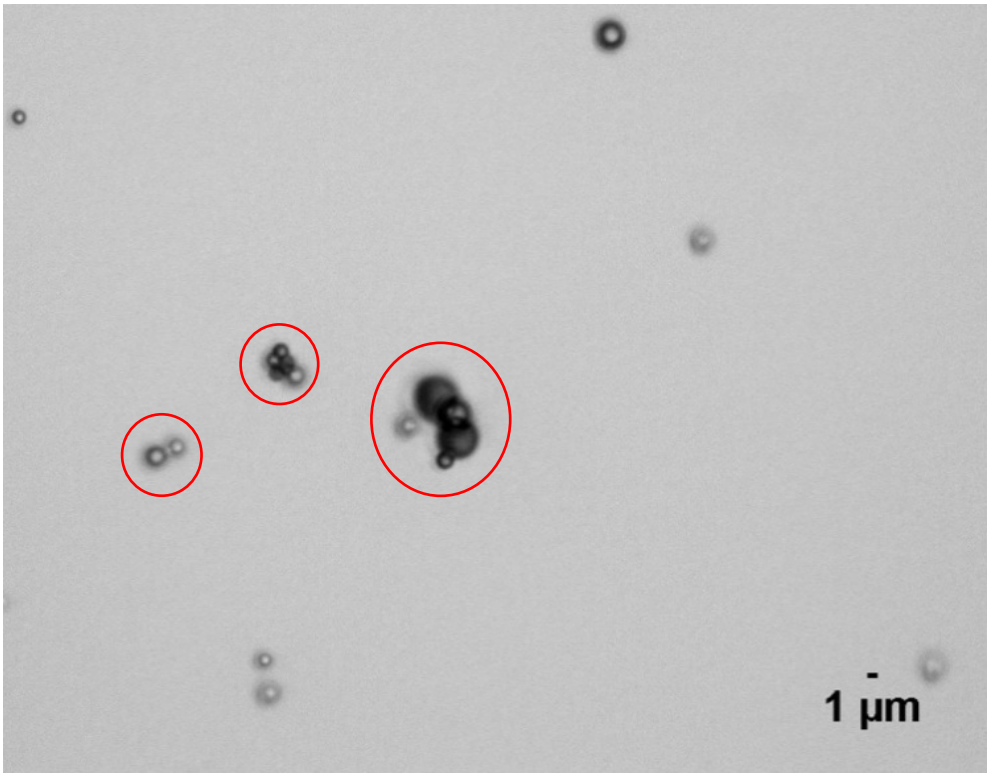

Figure 1a: Clusters observed in CCMCs under a microscope.

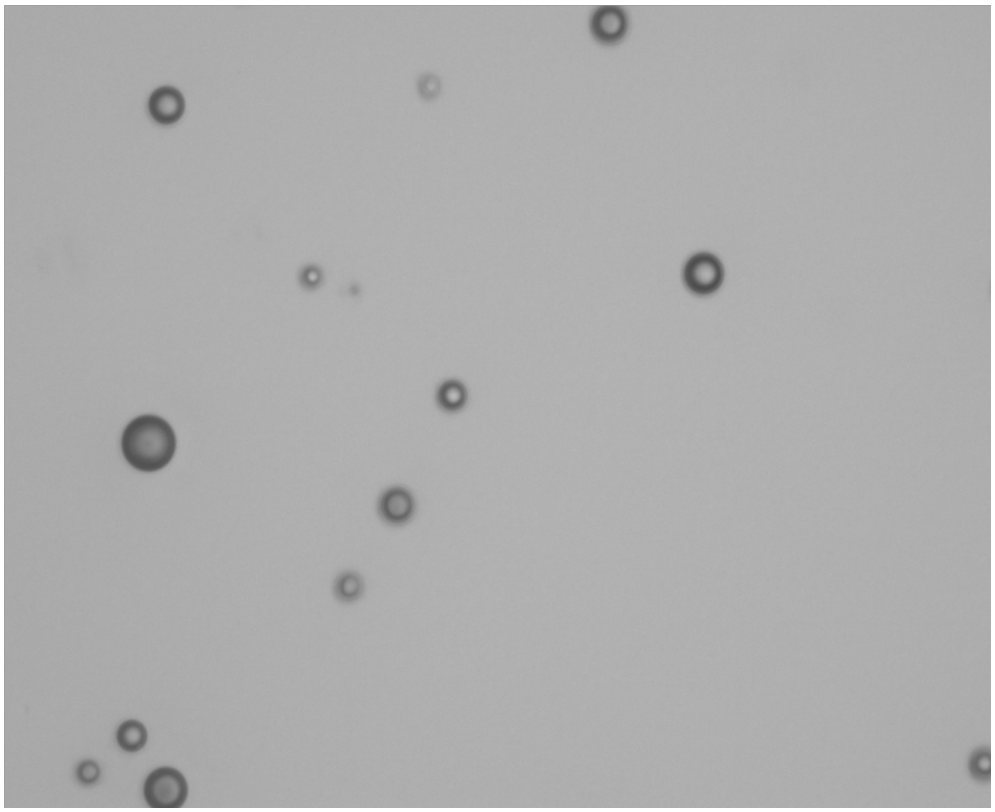

Figure 1b: Individual UCAs observed in negative control under a microscope.

2.2 Data collection using single element transducer and broadband hydrophone

Once the samples are validated under a microscope, RF data is captured using a 1.1 MHz focused ultrasound transducer (Olympus) to apply ultrasound and a 90º focally co-aligned broadband hydrophone (Sonics Concepts Y-107-MR) to receive the scattered signal. Figure 2 shows the acoustic setup used for collecting data. The 1.1 MHz transducer and hydrophone are aligned using a custom slide holder to reflect the transmitted signal directly to the broadband transducer. After alignment is complete, samples are diluted and dropped inside the acoustic chamber. The acoustic pressure and concentration of UCAs for both samples are kept constant. A time-series data is first collected for the negative control and followed by the CCMCs subsequently with a total of 7300 frames is captured and saved. Each dataset contains a total of 100 frames and a total of 73 different datasets were captured and converted to .MAT files for preprocessing.

2.3 Data collection using Verasonics system

After validating the samples for clusters and individual UCAs, RF data was collected using a GEM5ScD clinical phased array transducer and Verasonics Vantage 256 system (Verasonics, Redmond, WA). The samples were diluted with DI water. The concentration of UCAs and the acoustical pressure for both samples are kept constant to reduce external variations while collecting RF data. Figure 3 shows the flow phantom setup that is used. The phantom has two tunnels that run parallel to each other. Both the tunnels carry CCMCs and negative control respectively and they are exposed to ultrasound at the same time and the RF data of both the tunnels are captured together in a single frame. The complete process of collecting data for CCMCs and negative control is completed simultaneously. This reduces the variability in data of CCMCs and negative control that might occur while collecting datasets subsequently. A 20mL syringe is used to pump the solution through the phantom and was attached to a syringe pump set at a 1mL/min constant flowrate.

2.4 Data Preprocessing

The captured RF data went through a series of data preprocessing. For the data collection experiments as described below, the steps and conditions for data preprocessing were the same.

2.4.1 Data processing for single element transducer and broadband hydrophone datasets

Initial captured data was converted into MAT files using LabView. The MAT files were then sorted based on the number of frames. Each file had RF data of 100 frames and there were 73 files. Each file was created that consisted of 100 frames. These files were converted into datasets that had 1 frame in each. In total there were 14,600 samples with 7300 samples of CCMCs and negative control respectively. After loading the datasets into python, they were converted into NumPy arrays [11] and the two samples, CCMCs, and negative control were labeled into different classes. Using the scikit-learn library [12], the data was normalized and split into training and validation datasets.

2.4.2 Data processing for Verasonics dataset

The MAT files had 10,000 frames in one file and there were 105 files in total. A single element that is the central element for tunnel carrying CCMCs and the center element for the tunnel carrying negative control was saved into separate files. After separation of RF data for the two samples, they were loaded in python and converted into datasets that consisted of 1 frame. In total there were 1,660,000 samples of CCMCs and negative control respectively. These datasets were separated into classes and labeled as Class A and Class B. After normalizing the data using the scikit-learn library, they were split into training and validation datasets.

2.5 Deep Learning architecture

A simple artificial neural network (ANN)[13] was used for this classification task. Figure 4 shows a detailed description of the network architecture. The task here was to classify CCMCs and negative control with high accuracy. Classifying them into separate classes proves that the acoustic response of CCMCs is distinct and different from regular individual UCAs. To achieve this result, a simple ANN with 4 hidden layers with 20 units each and a RELU activation function was used (Fig 4). The labeled dataset was fed into the algorithm, with each sample point in the frame as an input. The output layer had one unit (two classes) with a sigmoid activation function. K-fold cross-validation technique[14] was used for avoiding overfitting of the data. We implemented the ANN in TensorFlow [15].

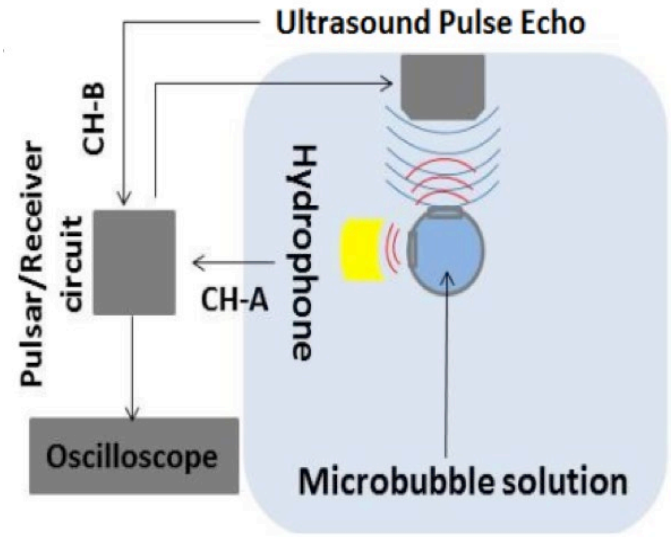

Figure 2: Acoustic chamber diagram with single element transducer and broadband hydrophone.

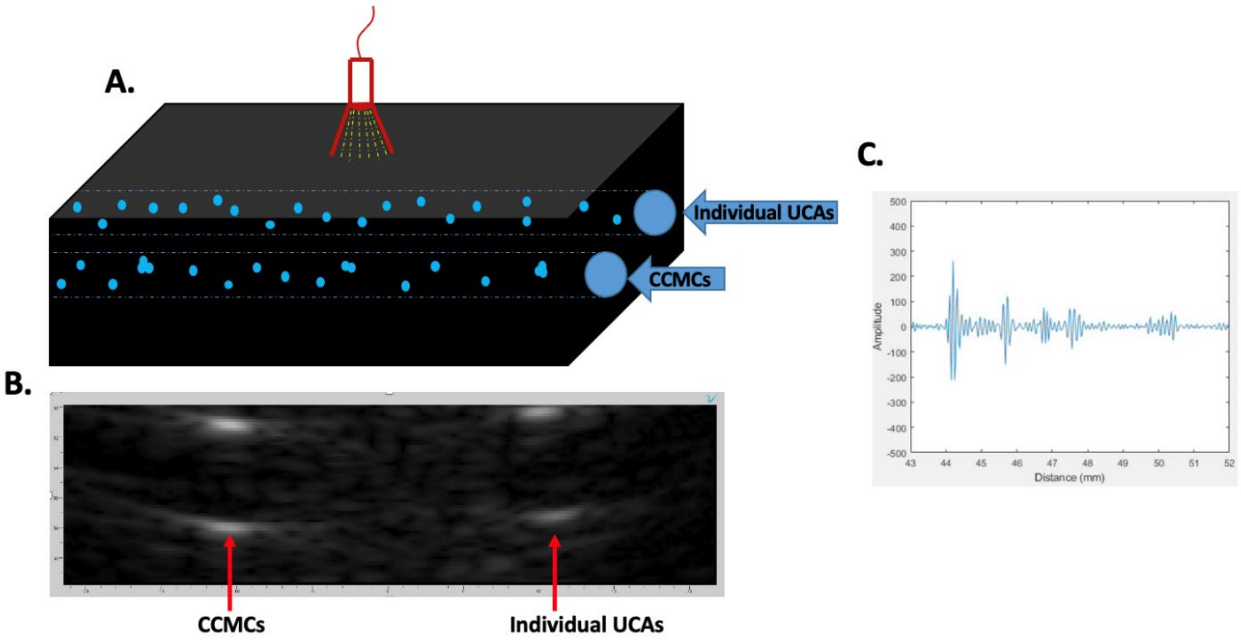

Figure 3a: Flow phantom setup. **3b:** 2D image from the Verasonics system. **3c:** Corresponding 1D RF data plot.

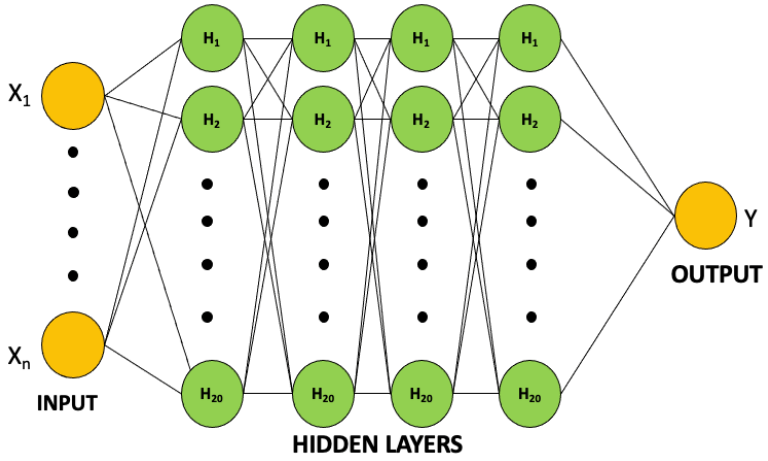

Figure 4: Network architecture with inputs X, 4 hidden layers, and 20 neurons each, and RELU activation function and output Y.

3. RESULTS

3.1 Training and validation results for a single element transducer and hydrophone dataset

We used the repeated k-fold cross-validation technique [14] for this task. We used ten folds and repeated it three times while randomizing the datasets for getting valid results without overfitting the model. A binary cross-entropy loss function [16] was used for calculating loss. The model was trained for a total of 100 epochs. The accuracy and loss can be observed in Figures 5a and 5b. The accuracies started at around 70% and reaches above 90% within 10 epochs. The model does not

take a lot of time to learn the distinction between the two datasets. The loss is minimized and reaches under 0.1 by the end of 50 epochs which shows that the model is optimized to classify the two datasets. We chose the model associated with the best training and validation accuracy, which was 98.6% and 95.2%, respectively. These results show that the RF data from the CCMCs and individual bubbles can be differentiated well with the help of a simple neural network model. The sudden variations in the validation accuracies and losses values are observed which might be due to changes in the weights for a certain model but it is improved immediately by optimizing the loss function.

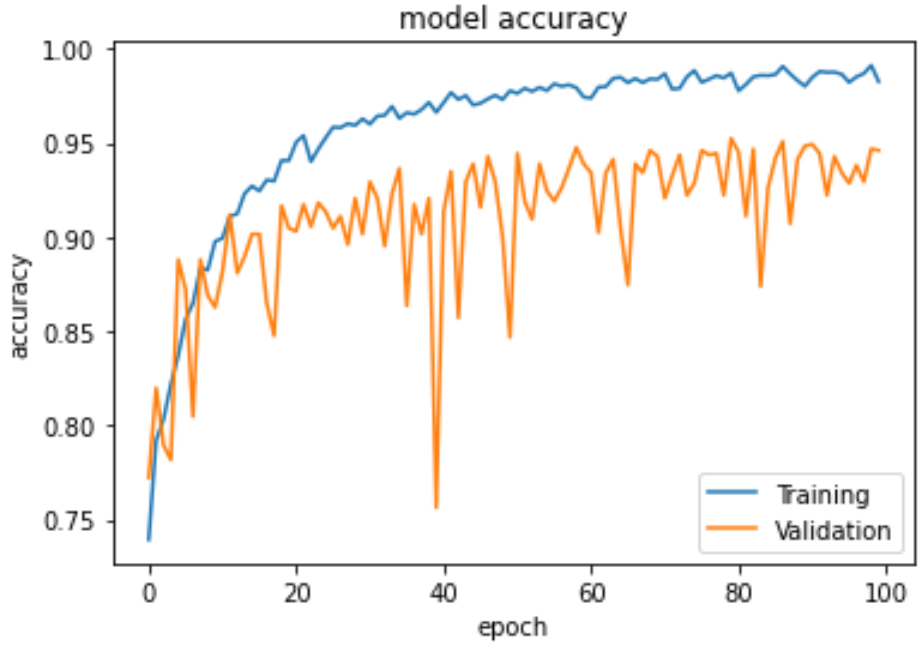

Figure 5a: Training and validation accuracies of broadband hydrophone data.

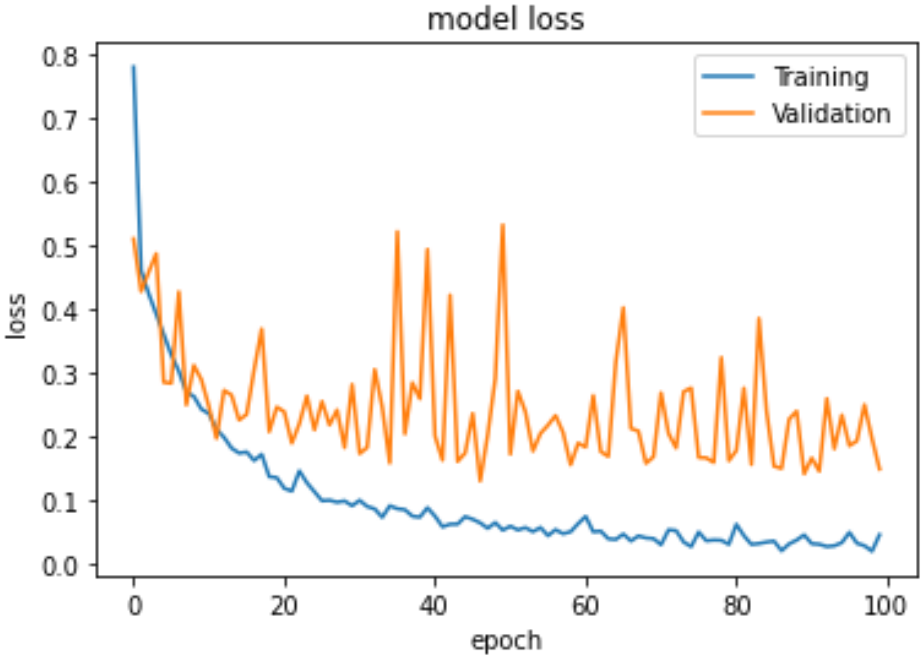

Figure 5b: Training and validation losses of broadband hydrophone data.

3.2 Training and validation results for Verasonics Datasets

We used a technique similar to what was used for the hydrophone data. The k-fold cross-validation technique utilizing 10 folds was used and repeated three times with randomization to avoid overfitting. A 100% training and validation accuracy was obtained with a simple four hidden layered ANN model. The results suggest the RF data of CCMCs, and negative control can be classified and distinguished between each other, showing that physically tethering bubbles together produces unique acoustic signatures detectable by a clinical transducer. The training and validation datasets were collected on different days using independently generated samples. The orientation of the transducer was changed occasionally to impart some variations in the dataset. The tunnels carrying UCAs were also swapped for the same reasons. With all these variations, the results achieved 100% training and validation accuracies (Figure 6a and 6b). The accuracy reached more than 90% at a very fast rate. The learning rate of the optimizer was reduced to stabilize the training process. The accuracy and loss curves are smooth as the training process is optimized. This suggests that the model is well trained to find the distinction between the two datasets even with the clinical transducer. To test the performance of the model, a new batch of the testing dataset was collected later by varying the orientation of the transducer and the tunnel carrying UCAs. This dataset was collected to show that the model was generalizable. The results for the testing dataset show us the performance of the model. An accuracy of 90.2% was achieved with high sensitivity and specificity of 90% and 84%, respectively, proving that there is a clear distinction between most of the datasets.

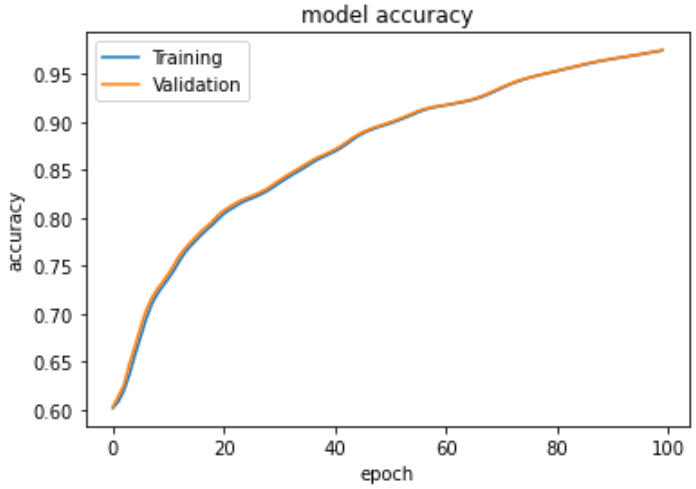

Figure 6a: Training and validation accuracies of clinical transducer RF data.

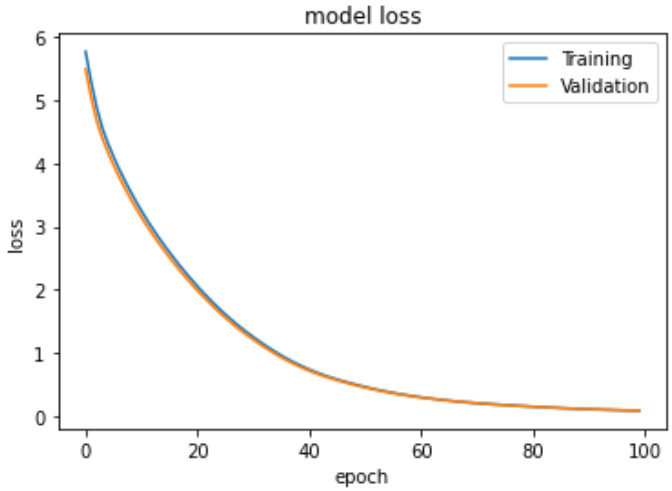

Figure 6b: Training and validation losses of clinical transducer RF data.

4. DISCUSSION AND CONCLUSION

The proposed method suggests the physical tethering of the lipid microbubbles, in the form of CCMCs, produces unique acoustic signatures compared to traditional UCAs. We anticipate that this unique acoustic response can be used to better distinguish CCMCs from background tissue and improve the sensitivity and accuracy of contrast agent detection *in vivo*. One area of future applications we are pursuing is to improve the diagnosis accuracy of small and centrally located lesions in prostate cancer using contrast-enhanced ultrasound imaging, where background signals can lead to misclassification of lesions. According to our hypothesis, during a coalescence event, the acoustic response of two microbubbles coalescing will be different from an individual microbubble oscillating volumetrically [17]. Based on this hypothesis, the coalescence event of CCMCs when exposed to low-intensity ultrasound can be one among many reasons for this distinction, although may not be the only factor that alters the acoustic response. One of the major tasks in our future work is to demonstrate conclusively that coalescence is responsible for the unique acoustic signatures and identify the part of the dataset that results in this classification between CCMCs and lipid UCAs. By understanding the precise acoustic differences between CCMCs and individual UCAs, we believe that the acoustics from individual CCMCs can then be identified, enabling more accurate spatial localization and 2D mapping on an ultrasound image. This has the potential to improve the signal-to-noise ratio (SNR) by suppressing the background noise. With better SNR, small lesions and centrally located lesions can be better localized and detected by imaging the micro-vascularity, with more precision and accuracy. This also has the potential to improve ultrasound super-resolution imaging with better detection and localization of novel contrast agents.

The results obtained for a single element transducer and broadband hydrophone are convincing, however, better accuracy can be obtained by using sophisticated deep learning algorithms that can perform better. We will collect more datasets and design a better ANN network architecture with more hidden layers. We did not use dropout layers for training our algorithm which can be used to improve the accuracy and used to optimize the results. Despite this, the results support the hypothesis that the acoustic response of CCMCs is sufficient to move forward with developing novel contrast agent detection techniques based on their unique response.

ACKNOWLEDGMENTS

This research was supported in part by the U.S. National Institutes of Health (NIH) grants (R01CA156775, R01CA204254, R01HL140325, and R21CA231911), by the Cancer Prevention and Research Institute of Texas (CPRIT) grant RP190588.

REFERENCES

[1] Sboros, V., Moran, C.M., Pye, S.D. & McDicken, W.N. The behaviour of individual contrast agent microbubbles. *Ultrasound in Medicine & Biology* **29**, 687-694 (2003).

[2] Ferrara, K.W., Borden, M.A. & Zhang, H. Lipid-shelled vehicles: engineering for ultrasound molecular imaging and drug delivery. *Acc Chem Res* **42**, 881-892 (2009).

[3] Qin, S., Caskey, C.F. & Ferrara, K.W. Ultrasound contrast microbubbles in imaging and therapy: physical principles and engineering. *Phys Med Biol* **54**, R27-57 (2009).

[4] Quaia, E. Microbubble ultrasound contrast agents: an update. *Eur Radiol* **17**, 1995-2008 (2007).

[5] Sirsi, S. & Borden, M. Microbubble Compositions, Properties and Biomedical Applications. *Bubble Sci Eng Technol* **1**, 3-17 (2009).

[6] Stride, E. & Saffari, N. Microbubble ultrasound contrast agents: a review. *Proc Inst Mech Eng H* **217**, 429-447 (2003).

[7] Gupta, I.*, et al.* Transrectal Subharmonic Ultrasound Imaging for Prostate Cancer Detection. *Urology* **138**, 106-112 (2020).

[8] Hall, R.L., Juan-Sing, Z.D., Hoyt, K. & Sirsi, S.R. Formulation and Characterization of Chemically Cross-linked Microbubble Clusters. *Langmuir* **35**, 10977-10986 (2019).

[9] Slagle, C.J., Thamm, D.H., Randall, E.K. & Borden, M.A. Click Conjugation of Cloaked Peptide Ligands to Microbubbles. *Bioconjug Chem* **29**, 1534-1543 (2018).

[10] Sirsi, S.R.*, et al.* Polyplex-microbubble hybrids for ultrasound-guided plasmid DNA delivery to solid tumors. *J Control Release* **157**, 224-234 (2012).

[11] Harris, C.R.*, et al.* Array programming with NumPy. *Nature* **585**, 357-362 (2020).

[12] Pedregosa, F.*, et al.* Scikit-learn: Machine Learning in Python. *J. Mach. Learn. Res.* **12**, 2825–2830 (2011).

[13] Pang, B., Nijkamp, E. & Wu, Y.N. Deep Learning With TensorFlow: A Review. *Journal of Educational and Behavioral Statistics* **45**, 227-248 (2020).
[14] Kohavi, R. A study of cross-validation and bootstrap for accuracy estimation and model selection. in *Proceedings of the 14th international joint conference on Artificial intelligence - Volume 2* 1137–1143 (Morgan Kaufmann Publishers Inc., Montreal, Quebec, Canada, 1995).
[15] Abadi, M.*, et al.* TensorFlow: A system for large-scale machine learning. in *OSDI* (2016).
[16] Murphy, K.P. *Machine learning: a probabilistic perspective*, (MIT press, 2012).
[17] Postema, M., Marmottant, P., Lancee, C.T., Hilgenfeldt, S. & de Jong, N. Ultrasound-induced microbubble coalescence. *Ultrasound Med Biol* **30**, 1337-1344 (2004).